Scanning Hall probe microscopy

A. M. Chang, H. D. Hallen, L. Harriott, H. F. Hess, H. L. Kao, J. Kwo, R. E. Miller, R. Wolfe,[a] and J. van der Ziel[b]
AT&T Bell Laboratories, Murray Hill, New Jersey 07974

T. Y. Chang
AT&T Bell Laboratories, Holmdel, New Jersey 07733

(Received 5 June 1992; accepted for publication 18 August 1992)

We describe the implementation of a scanning Hall probe microscope of outstanding magnetic field sensitivity ($\sim$0.1 G) and unprecedented spatial resolution ($\sim$0.35 μm) to detect surface magnetic fields at close proximity to a sample. Our microscope combines the advantages of a submicron Hall probe fabricated on a GaAs/$Al_{0.3}Ga_{0.7}As$ heterostructure chip and the scanning tunneling microscopy technique for precise positioning. We demonstrate its usefulness by imaging individual vortices in high T_c $La_{1.85}Sr_{0.15}CuO_4$ films and superconducting networks, and magnetic bubble domains.

Many methods have been invented to detect the surface magnetic field at close proximity to a sample surface. These include Hall probe,[1] Faraday rotation,[2] electron holography,[3] magnetic decoration (bitter pattern),[4] and magnetic force microscopy (MFM)[5] techniques. However, to date, none has achieved the combined desirable characteristics of quantitative measurement of the magnetic field, good spatial resolution, and noninvasiveness. In this letter, we describe a specific implementation of a scanning Hall probe microscope (SHPM)[6] which provides excellent field sensitivity and spatial resolution an order of magnitude better than previous Hall probe microscopes. Our microscope contains a Hall probe which can be precisely positioned at close proximity to yield information about local magnetic field profile in the direction normal to the sample surface. Unlike the MFM technique, the Hall probe exerts negligible force on the underlying magnetic structure and is noninvasive, and unlike the magnetic decoration technique, the same area can be scanned over and over again. Many potential applications are possible, such as the study of surface magnetic memory devices, or the magnetic field profile due to vortices in superconducting films, networks, or crystals, spatially varying current flow in patterned microstructures, or domain structures near surfaces in magnetic systems. Thus far, we have succeeded in imaging micron-size magnetic bubble domains in thin magnetic bubble Garnate ($YGdTmFe_{4.2}Ga_{0.8}O_{12}$) films, where the surface field is of order 400 G, at a temperature of 86 K. More spectacularly, individual vortices at the surface of c-axis $La_{1.85}Sr_{0.15}CuO_4$ high T_c films with $\sim$10 G surface fields, were imaged below the T_c of $\sim$28 K, enabling us to extract the penetration depth of a single vortex.

To achieve the desired characteristics, our SHPM takes advantage of the magnetic field sensitivity and spatial resolution offered by a submicron GaAs/$Al_xGa_{1-x}As$ heterostructure Hall bar, and the precision-positioning capability offered by the scanning tunneling microscopy (STM) technique. The Hall bar has a field resolution of $\sim$0.36 G/$\sqrt{\text{Hz}}$ under optimal operating conditions of low temperature ($T\sim$4.2 K), a spatial resolution of $\sim$0.35 μm, and can be positioned to within 0.2 μm of the sample surface. The microscope geometry comprises of a Hall bar patterned within 4 μm of one corner of a GaAs/$Al_{0.3}Ga_{0.7}As$ heterostructure chip, mounted onto a standard low temperature STM stage with its normal along the z axis of the stage as illustrated in Fig. 1. Close proximity to the surface of a sample is achieved by adjusting the surface relative to the Hall probe chip to a shallow angle of approximately 1°. To locate the sample surface a standard tunneling technique is employed, and for this purpose the corner of the Hall probe chip is coated with a thin layer of gold and serves as the tunneling tip.

The Hall bar pattern contains a main current channel which runs diagonally away from the corner of the GaAs/$Al_{0.3}Ga_{0.7}As$ chip, with two Hall junctions spaced 2 μm apart. The junction closer to the corner is $\sim$4 μm from the rounded corner as shown in Fig. 2(a). The lithographic linewidth is 0.5 μm. Due to surface depletion however, the conducting width is typically about 0.15 μm in the straight section, and the Hall junction region is $\sim 0.35\times 0.35$ μm^2 in area. Fabrication starts from a 5×5 mm^2 piece of material from which four independent Hall bars on 2.5×2.5 mm^2 chips will be produced. The finished Hall bars are $\sim$35 μm from the corner of the cleaved chips. A deep ($\sim$2.5 μm) etch serves to bring the tunnel touch down point to within 4 μm of the Hall bar (the top of the cliff) rather than the actual corner of the chip as is seen in Fig. 2(b).

The fabrication consists of the following steps: (1) contact alloying, (2) electron beam lithography to define the submicron Hall bar pattern, (3) metallization and liftoff to create the submicron etch mask, (4) photolithography and wet chemical etch to define the lead pattern extending the submicron features to the contacts, (5) cliff lithography and deep etch, (6) lead protection photolithography and final shallow etch to isolate and define the submicron pattern, and (7) laser precision cleave into four independent Hall bar chips. The details of the electron beam lithography and chemical etching can be found in Ref. 7.

[a]Presently associated with AT&T Corporate, Liberty Corner, NJ 07059.
[b]Present address: University of Texas at Dallas, Richardson, TX 75083.

 0003-6951/92/411974-03$03.00

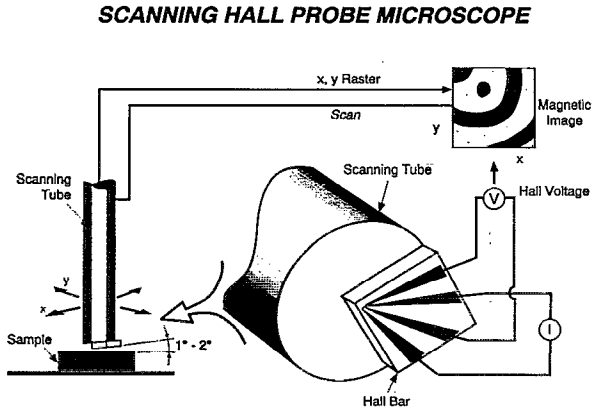

FIG. 1. A schematic of the scanning Hall probe microscope.

The $GaAs/Al_{0.3}Ga_{0.7}As$ material we chose has a low mobility of 50 000 cm^2/V s and a density of 2×10^{11} cm^{-2}. The low mobility samples do not exhibit the quenching of the Hall effect[8] associated with ballistic transport in the junction. Typical Hall coefficients obtained at 4.2 K are about 0.4 Ω/G, slightly higher than the conventional value of 0.33 Ω/G for this density.

The construction of the scanning apparatus uses many standard techniques of STM.[9] The Hall bar is attached to the end of a PZT-8 piezoelectric scanning tube which has a 6 μm range at 4 K temperature. The sample is mounted below on a tiltable platform and adjusted so that a 1°–2° angle exists between it and the plane of the chip with the Hall bar corner in closest proximity. The whole assembly is mounted on a cryostat with a 1.3 K temperature pumped liquid helium pot and inserted into a superconducting magnet. The need to approach the sample surface in the shallow angle geometry dictates that all surfaces must be flat and free of debris. Coarse approach is achieved with a differential spring mechanism driven by a cryogenic stepper motor. The position and plane of the surface is determined by tunneling and the plane of the scan is set parallel to and 600 Å back from the surface.

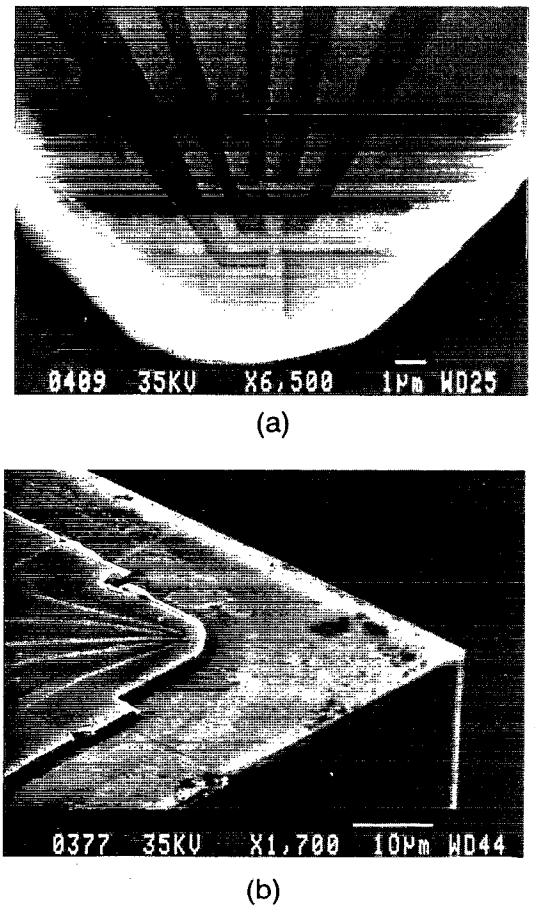

FIG. 2. Electron micrographs of the (a) Hall bar showing the front and back Hall junctions and the rounded corner which serves as the tunneling tip. (b) The cliff structure of the Hall probe chip corner.

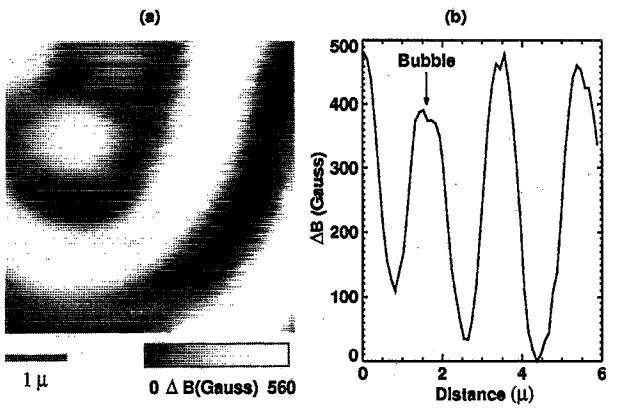

FIG. 3. (a) A 4.5×4.5 μm^2 scan image of the normal magnetic field component at 0.22 μm above a 0.8 μm thick $YGdTmFe_{4.2}Ga_{0.8}O_{12}$ bubble Garnate film. Note the presence of bubble-like and lamellar line domain structures. (b) A line cut of the image in (a) along the 45° diagonal from top left to bottom right. The bubble domain as indicated by the arrow is about 0.92 μm in size.

For many measurements (e.g., determining the penetration depth λ) it is important to know the distance between the Hall bar and the sample accurately. The closest distance to the sample surface is determined by three factors: (1) the horizontal distance between the tunneling point to the Hall bar junction which is about 4 μm from the front bar and 6 μm for the back bar, (2) the angle of mounting of the sample which is approximately 1°, and (3) the depth at which the conducting electrons are buried beneath the gold-coated top surface of the $GaAs/Al_{0.3}As_{0.7}As$ chip which is about 0.11 μm. Together, they yield a minimum height of 0.17 and 0.22 μm for the two Hall bars. Since the magnetic field features due to small structures rapidly wash out at heights exceeding the typical size or spacing between structures, the minimum height also serves as a limiting factor to the spatial resolution, in addition to the intrinsic size of the Hall junction.

We have used the technique to image part of a magnetic bubble garnet film[10] which, when properly magnetized, exhibits magnetic domains shaped either like bubbles (cylinders) or lamellar-type lines with the smallest dimension of order the film thickness (0.8 μm for the film used here). An image showing both types of structure is shown in Fig. 3(a). The sample was prepared with mixed bubbles and lines then imaged in zero applied field. The 4.5×4.5

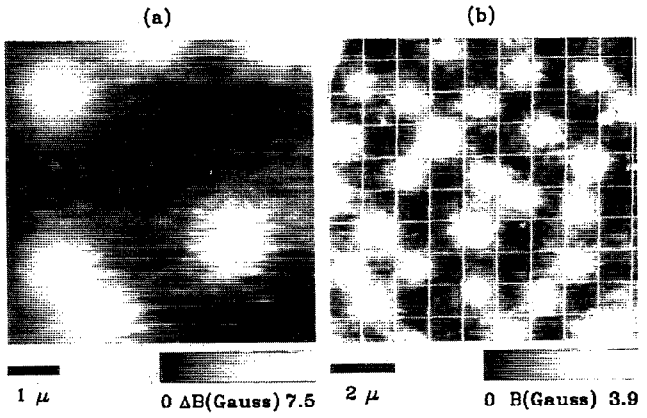

FIG. 4. (a) A 5×5 μm^2 scan of the normal magnetic field component at 0.25 μm above a c-axis $La_{1.85}Sr_{0.15}CuO_4$ film of 0.8 μm thickness. The roughly circular, whitish features represent individual vortices of flux $\sim hc/2e$. The film was field cooled in a 5 G magnetic field and imaged at 4.2 K temperature. The superconducting transition occurs at 28 K. (b) 9.3×9.5 μm^2 image from a Nb square grid sample. The white lines delineate the expected grid positions and the squares with whiter interiors are grid holes populated by one vortex.

μm^2 image was acquired at a temperature of 86 K and shows structures of $\sim$400 G in amplitude. The size of the bubbles in the image is 0.92 μm as is evident in the line cut taken from the image through the center of the lower bubble slanting 45° downward, which is shown in Fig. 3(b). Contributions to the transition width between domains arise from the inherent magnetic structure dimension, the Hall bar size, and the spreading of the magnetic field at the Hall bar height position of 0.22 μm above the sample.

The magnetic field which passes through thin superconducting films cooled below the transition temperature is well known to bunch up into bundles (vortices each containing a single quantum of magnetic flux $\Phi_0=hc/2e$ $=20.7$ G μm^2. Thus far, these vortices have been imaged primarily by the bitter pattern technique.[11] Figure 4 shows a magnetic image 0.25 μm above a high temperature superconducting (HTSC) $La_{1.85}Sr_{0.15}CuO_4$ film grown by off-axis sputtering.[12] The 0.8 μm thick film was grown with the c-axis normal, has a $T_c\sim28$ K, and was imaged at 4.2 K subsequent to field cooling in a 5 G field. The roughly circular features in the image are individual vortices containing a single flux quantum verified by integrating the field amplitude over a region of the image to obtain $\sim\Phi_0$. The lateral extent of the vortices is governed by the magnetic penetration depth λ of the local superconducting material. For the HTSC materials, λ is large which allows us to extract it directly from the images via the London equation without a large correction for the Hall bar size. The resulting cylindrically symmetric boundary value problem can be reduced to a numerical integration for the field at each point,[13] although care must be taken to account for the spreading of the fields above the surface of the superconductor, and film thickness (d) effects when $\lambda > \sim d$.

By expanding the terms in the integral expression of Ref. 13 for the z component of the field B_z for the distances $(r^2+z^2)^{1/2}\gg\lambda$, where r is the radial distance and z is in the direction of the surface normal, one finds, to first order, that the field profile resembles that of a monopole situated $\lambda_{\rm eff}$ below the surface:

$$B_z=\frac{\Phi_0}{2\pi}\frac{z+\lambda_{\rm eff}}{[r^2+(z+\lambda_{\rm eff})^2]^{3/2}}, \tag{1}$$

where $\lambda_{\rm eff}=\lambda\coth(d/2\lambda)$. $\lambda_{\rm eff}$ differs appreciably from λ when the film is so thin that the vortex core is not well formed. For the upper left, lower right and two lower left vortices in Fig. 4(a) we obtain $\lambda=3426$, 3455, and 3933 Å using the monopole model, and $\lambda=3408$, 3427, and 4049 Å fitting with the exact model. The fitting models take into account the Hall bar size by convolving the calculated field profile with a square the size of the Hall bar. For isolated vortices, a simple estimate of λ can be obtained from the magnitude of B in the center of the vortex yielding 3503, 3373, and 3358 Å, respectively.

As a final example, insight can be gained into model systems of superconducting networks where vortex configuration is the subject of intense interest. Here the sample is a 1000 Å niobium film that has been milled into a square grid pattern with 1 μm spacing of 0.5 μm holes using a gallium focused ion beam. The magnetic field was set so that roughly 0.3 grid sites were filled. A checkerboard network of vortices minimizes the free energy at half filling. This is observed in parts of the image presented in Fig. 4(b), and shows how this technique can be used to probe the ground state configuration of such a system.

In summary, we have developed a scanning Hall probe microscope which detects surface magnetic fields with excellent sensitivity at close proximity to the sample. We have demonstrated the ability to image magnetic domain structures in bubble garnate films, individual vortices in high T_c superconductor films, and extracted the local penetration depth, and vortices in superconducting networks.

[1] H. T. Coffey, Cryogenics 7, 73 (1965); R. N. Goren and M. Tinkham, J. Low Temp. Phys. **5**, 465 (1971).
[2] P. B. Alers, Phys. Rev. **105**, 104 (1957).
[3] T. Matsuda, A. Fukuhara, T. Yoshioka, S. Hasegawa, A. Tonomura, and Q. Ru, Phys. Rev. Lett. **66**, 457 (1991).
[4] H. Traeuble and U. Essmann, J. Appl. Phys. **25**, 273 (1968); G. J. Dolan, F. Holtzberg, C. Field, and T. R. Dinger, Phys. Rev. Lett. **62**, 2184 (1989).
[5] Y. Martin, D. Rugar, and H. K. Wickramasinghe, Appl. Phys. Lett. **52**, 244 (1988).
[6] A similar approach has been taken by M. A. Itzler, J. A. Simmons, and P. M. Chaikin, Bull. Am. Phys. Soc. **36**, 724 (1991) employing a 1×1 μm^2 Hall bar, without the STM positioning capabilities.
[7] K. Owusu-Sekyere, A. M. Chang, and T. Y. Chang, Appl. Phys. Lett. **52**, 1246 (1988).
[8] M. L. Roukes, A. Scherer, S. J. Allen, H. G. Craighead, R. M. Ruthen, E. D. Beebe, and J. P. Harbison, Phys. Rev. Lett. **59**, 3011 (1987).
[9] J. Stroscio, Ed., *Scanning Tunneling Microscopy* (Academic, New York, 1992).
[10] A. H. Bobeck and H. E. D. Scovil, Scientific American **224**, No. 6, 78 (1971); J. C. North and R. Wolfe, in *Ion Implantation in Semiconductors and Other Materials*, edited by B. L. Crowder (Plenum, New York, 1973), p. 505.
[11] P. L. Gammel, D. J. Bishop, G. J. Dolan, J. R. Kwo, C. A. Murray, L. F. Schneemeyer, and J. V. Waszczak, Phys. Rev. Lett. **59**, 2592 (1987).
[12] H. L. Kao, J. Kwo, R. M. Flening, M. Hong, and J. P. Mannaerts, Appl. Phys. Lett. **59**, 2748 (1991); J. Kwo, R. M. Fleming, H. L. Kao, D. J. Werden, and C. H. Chen, Appl. Phys. Lett. **60**, 1905 (1992).
[13] A. M. Chang, H. D. Hallen, H. F. Hess, H. L. Kao, J. Kwo, A. Sudbo, and T. Y. Chang (unpublished).